

Interrogations of Direct Numerical Simulation of Solid-Liquid Flow

Daniel D. Joseph
University of Minnesota
107 Akerman Hall
110 Union Street SE
Minneapolis, MN 55455

Table of Contents

Abstract	1
I Introduction.....	1
▪ What is DNS?.....	1
▪ Approximate Methods	2
▪ Data Structure for Applications of DNS	3
II Equations of Motion.....	4
▪ Weak Solution for the Total Momentum	4
III Numerical Packages for Moving Particles in Direct Numerical Simulation.....	6
▪ ALE Particle Mover.....	6
▪ A Projected Particle Mover	7
▪ DLM Particle Mover	7
▪ Parallel Implementation	9
▪ Viscoelastic DLM Particle Mover	10
▪ Computation domains for pipe flows of slurries	10
▪ Collision Strategies.....	11
IV Weak and Strong Formulations of the DLM Method.....	13
▪ Body Force Formulation of DLM Method: Weak Solution	13
▪ Body Force Formulation of DLM: Strong Solutions	13
▪ Stress Formulation of DLM: Weak Solutions	15
▪ Stress Formulation of DLM: Strong Solutions.....	16
▪ Addendum to Chapter IV (Addendum A). Weak form of body force formulation when the Lagrange Multiplier is eliminated	A.1
V Applications of DNS.....	17
▪ Studies of Microstructure.....	17
▪ Sedimentation and Fluidization.....	20
▪ Mechanisms of Cross-Stream Migration	21
▪ Slot Problems for Particle Transport in Fractured Reservoirs	23
▪ Lift-off, Resuspension, Equilibrium Height, Slip Velocities, Lift-Force Ratios.....	24
VI Modeling and DNS	25
▪ Averaging	25
▪ Fluidization by Drag and Fluidization by Lift	30
▪ Fluidization and Sedimentation.....	30
▪ Two Differences Between Fluidization and Sedimentation	31
▪ Uniform Fluidization	31

▪ Incipient Fluidization.....	32
▪ Hindered Settling.....	33
▪ Drag and Hindered Settling.....	36
▪ Dynamic and One Dimensional Models	38
▪ Particle Phase Pressure and the Stability of Uniform Fluidization	39
VII Direct Numerical Simulation of Fluidization of 1204 Spheres.....	41
▪ Experiments	41
▪ Numerical Method.....	41
▪ Experiments	44
▪ Numerical Simulation.....	46
▪ Qualitative comparison of experiment and simulation	49
▪ Numerical computation of averaged quantities	52
▪ Dynamic and wall friction pressure in a fluidized bed.....	55
▪ Sedimentation and fluidization velocity of single spheres	57
▪ Richardson-Zaki correlations from DNS	60
▪ Discussion.....	63
VIII Modeling Rayleigh-Taylor instability of a sedimenting suspension of circular particles.....	65
▪ Simulation Data.....	65
▪ Comparison of Two-fluid Model and Simulation	71
▪ Discussion and Conclusions	74
IX Fluidization by lift: single particle studies.....	85
▪ Equations of motion and dimensionless parameters	86
▪ Lift-off of a single particle in plane Poiseuille flows of a Newtonian fluid	89
▪ Data Structure for DNS and experiments.....	95
X Analytical models of lift	100
▪ Lift in an inviscid fluid	100
▪ Low Reynolds numbers	102
▪ Lift in shear flows at low R	104
▪ Slip velocity and lift	105
▪ Non-uniqueness.....	106
▪ Validation of lift formulas by DNS	107
▪ Wall effects in shear flows.....	109
▪ Curvature	110
▪ Regular perturbation in the wall region	111
▪ Reciprocal theorem.....	113
▪ Finite size sphere near a wall	114
XI Slip velocity and lift at finite Reynolds numbers.....	118
▪ Equilibrium positions of neutrally buoyant and heavy particles.....	118
▪ Mechanism for lift	119
▪ Numerical simulation of migration and lift.....	120
▪ Long particle model.....	121
▪ Slip velocities, angular slip velocities and lift for neutrally buoyant circular particles.....	127
▪ Slip velocities, angular slip velocities and lift for non-neutrally buoyant circular particles.....	130
▪ Summary.....	134
XII Stability and turning point bifurcations of a single particle in Poiseuille flow.....	136
▪ Pressure lift and shear lift	143

XIII	Lift off of a single particle in plane-Poiseuille flow of an Oldroyd-B fluid	149
▪	Neutrally buoyant particle.....	150
▪	Pressure shear and viscoelastic lift forces	154
▪	Power law correlations for lift-off in an Oldroyd B fluid.....	158
XIV	Fluidization by lift of 300 circular particles in plane Poiseuille flow by DNS	163
▪	Case 1: $\eta = 1$ poise, $R_G = 9.81$	164
▪	Case 2: $\eta = 0.2$ poise, $R_G = 245$	171
▪	Case 3: $\eta = 0.1$ poise, $R_G = 9.81/\eta^2 = 9.8 \times 10^3$	177
▪	Case 4: $\eta = 0.05$ poise, $R_G = 9.81/\eta^2 = 3.92 \times 10^4$	186
▪	Case 5: $\eta = 0.01$ poise, $R_G = 9.81/\eta^2 = 9.8 \times 10^4$	194
▪	An engineering correlation for the lift-off of circular particle in a plane Poiseuille flow of a Newtonian fluid.....	199
▪	Inertial mechanism of fluidization.....	202
XV	Bi-power law correlations for sediment transport in pressure driven channel flows	207
▪	Analogy between fluidization by drag and lift	207
▪	Direct numerical simulation (DNS) of solid-liquid flows	209
▪	Experimental setup	211
▪	Experimental correlations for sediment transport.....	213
	Dimensionless parameters	213
	Power law correlations for the erosion case (Patankar et al. 2002).....	213
	Bi-power law correlations for the bed load transport case (Wang et al. 2002)	215
▪	Summary.....	227
▪	Appendix A (contribution of B. Baree).....	229
	Fitting power-law data with transition regions by a continuous function: General framework and application to the Richardson-Zaki correlation	229
▪	Appendix B	233
XVI	Epilogue.....	234
▪	Acknowledgment	237
	References	238
	Nonmenclature list	249
	Index	252

Abstract

In direct simulation the fluid motion is resolved numerically and the forces which move the particles are computed rather than modeled. This procedure opens new windows for understanding and modeling. Numerical methods are discussed based on body fitted moving unstructured grids and another on a fixed grid in which the portions of the fluid occupied by solids are forced to move as a rigid body by a distribution of Lagrange multipliers. Animation of the fluidization of 1204 spheres in 3D will be compared with experiments and the concept of fluidization of slurries in conduits by lift rather than drag will be framed in animation by direct simulation. Correlation for lift-off of single particles and the bed height of slurries fluidized by lift are obtained by processing data from numerical experiments.

I. Introduction

The current popularity of computational fluid dynamics is rooted in the perception that information implicit in the equations of motion can be extracted without approximation using direct numerical simulation (DNS).

▪ What is DNS?

Direct numerical simulation of solid-liquid flows is a way of solving the initial value problem for the motion of particles in fluids exactly, without approximation. The particles are moved by Newton's laws under the action of hydrodynamic forces computed from the numerical solution of the fluid equations.

To perform a direct simulation in the above sense, therefore, one must simultaneously integrate the Navier-Stokes equations (governing the motion of the fluid) and the equations of rigid-body motion (governing the motion of the particles). These equations are coupled through the no-slip condition on the particle boundaries, and through the hydrodynamic forces and torques that appear in the equations of rigid-body motion.

These hydrodynamic forces and torques must of course be those arising from the computed motion of the fluid, and so are not known in advance, but only as the integration proceeds. It is crucial that no approximation of these forces and torques be made--other than that due to the numerical discretization itself--so that the overall simulation will yield a solution of the exact coupled initial value problem--up to the numerical truncation error.

Our goal is to do direct numerical solutions with many thousands of particles in three dimensions, with large volume fractions, for the various kinds of suspensions and slurries that model the practical particulate flows arising in applications like fluidized beds, slurry transport, transport of drill cuttings for oil production, and proppant sands in reservoir stimulations. In this article, we present the results of a simulation of the fluidization of 1204 spheres and other simulations for targeted applications.

The hope is that the direct simulation of the motions of thousands of particles will, in many cases, allow the large numbers of experiments used in deriving engineering correlations to be replaced by cheaper, safer numerical experiments in which flow, material, and process-control parameters can be altered with a computer command. With DNS you can turn physical factors on or off to isolate effects, which is something that cannot be done in experiments. There are also opportunities for the application of direct simulation to the diagnosis of industrial problems involving flowing particulates, to the establishment of benchmark standards for two-phase flow models (see Chapter VI), and to approximate numerical methods that track particles.

▪ **Approximate Methods**

The signal feature of approximate numerical methods which track particles is that the forces that the fluid exerts on the particle are modeled rather than computed as in DNS. Many excellent numerical studies of particulate flows of many particles which are not direct simulations in the above sense have appeared in recent years. These approximate methods include simulations based on potential flow, Stokes flow, and point-particle approximations. They all simplify the computation by ignoring some possibly important effects like viscosity and wakes in the case of potential flow; inertial forces which produce lateral migration and across-the-stream orientations in the case of Stokes flow; and the effects of stagnation and separation points in the case of point-particle approximations.

Particle tracking methods take into account the particles and the fluid motion to understand particulate flow. Particle tracking methods move the particles by Newton's equations for rigid bodies using forces that are modeled from single particle analysis or from empirical correlation rather than from forces which are obtained by direct computation from the fluid motion. This kind of simulation is called Lagrangian because the particles are tracked. The fluid motion in particle tracking methods are computed from field equations, like the Navier-Stokes defined at every point of the field including points occupied by the particles. This kind of computation from continuum partial differential equations on a field is called Eulerian; hence, particle tracking methods are Eulerian-Lagrangian. The particle tracking can have a one way coupling in which the fluid motion is computed without particles, and a two-way coupling in which some effects of the particle motion on the fluid motion are recognized. In most cases the two-way coupling is introduced by momentum exchange terms representing the force of the particles on the fluid. A more general coupling was introduced by Andrews and O'Rourke 1996 and Snider, O'Rourke and Andrews 1998. They presented a scheme that considers the particle phase both as a continuum and a discrete phase. Inter-particle stresses are calculated by treating the particle as a continuum phase, as in the fluid phase equations of a two-fluid model. This way, they can track the motion of the particles and at the same time model the inter-particle stress. In their scheme the viscosity of the fluid in the fluid phase is neglected. The method can handle particulate loading ranging from dense to dilute, and particles of different size and materials. The particles are grouped into parcels. The motion of the parcels is tracked by the Lagrangian approach. The number of parcels in a computational cell are used to calculate the solid phase volume fraction on the Eulerian grid. Patankar and Joseph 1999, 2001 have extended this kind of particle-in-cell method to account for fluid phase viscosity and other effects.

The problem of particles in turbulent flows has been treated using turbulent flow models for the fluid with one-way coupling and two-way coupling with momentum exchange applicable to

dilute mixtures. These kind of turbulent flow models have been discussed by McLaughlin 1994 in a comprehensive review paper. Some of these turbulent flow models are conventionally called DNS; they are not DNS for particulate flow in that the forces on the particles are modeled and not computed from the fluid motion.

Another method used to compute solid-liquid is the Lattice Boltzmann method (LBM). This is an unconventional computational approach that constructs simplified kinetic models for the motion of discrete fluid particles. The LBM is inspired by Boltzmann's equation which give rise to the Navier-Stokes equations at 2nd order in Chapman-Enskog expansion and to Burnett equations, which do not agree with experiments at 3rd order. The LBM gives rise to equations for a compressible fluid, which are Navier-Stokes-like but not Navier-Stokes equations (see Qian, d'Humieres and Lallemand 1992, Ladd 1994, How, Zou, Chen, Doolen and Cogley 1995, Chen and Doolen 1998). The LBM may give rise to good approximations of isochoric flow when the pressure gradients are not too large. For large pressure gradients the fluid will compress. The LBM gives rise to particulate flows that are close to those computed by DNS (see Ladd 1997; Aidun, Lu and Ding 1995, and Qi 1999). The good results achieved by LBM probably arise from the fact that the forces on particles for this method are computed rather than modeled.

▪ Data Structure for Applications of DNS

DNS generates huge amounts of data. It is necessary to post-process the data to get useful results. The way the data is generated and processed is determined by the application; to interrogate the data efficiently it is necessary to create a *data structure for post processing*. The problem of setting up a data structure for the interrogation of results of simulations is a way of determining the way that numerical simulations ought to be applied; it connects the computational world to the applications.

The literature of DNS is by now fairly extensive. This literature is listed chronologically in chapter IV. This same literature, together with the paper abstracts and animations of computer simulations, can be found on our web page http://www.aem.umn.edu/Solid-Liquid_Flows.

II. Equations of Motion

The equations to be solved in the case of a Newtonian fluid are as follows. In the fluid we have

$$\nabla \cdot \mathbf{u} = 0 \quad (\text{II.1})$$

and

$$\rho_f \left(\frac{\partial \mathbf{u}}{\partial t} + (\mathbf{u} \cdot \nabla) \mathbf{u} \right) = \rho_f \mathbf{g} - \nabla p + \eta \nabla^2 \mathbf{u}. \quad (\text{II.2})$$

For simplicity of presentation we consider spherical particles. The mass center of the spheres are at $\mathbf{X}(t)$. The particles equations of motion are

$$\begin{aligned} M \frac{d\mathbf{U}}{dt} &= M\mathbf{g} + \mathbf{F}[\mathbf{u}], & I \frac{d\boldsymbol{\omega}}{dt} &= \boldsymbol{\mathcal{T}}[\mathbf{u}] \\ \frac{d\mathbf{X}}{dt} &= \mathbf{U}, & \frac{d\boldsymbol{\theta}}{dt} &= \boldsymbol{\omega}, \end{aligned} \quad (\text{II.3})$$

where $\mathbf{F}[\mathbf{u}]$ is the force and $\boldsymbol{\mathcal{T}}[\mathbf{u}]$ the torque on the particle. The fluid velocity is the same as the particle velocity at the surface of the particle

$$\mathbf{u} = \mathbf{U} + \boldsymbol{\omega} \wedge \mathbf{r}. \quad (\text{II.4})$$

The fluid force $\mathbf{F}[\mathbf{u}]$ acting on the boundary of the particle is the integral over the body surface of the traction

$$\boldsymbol{\sigma} \cdot \mathbf{n} = -p\mathbf{n} + 2\eta \mathbf{D}[\mathbf{u}] \cdot \mathbf{n} \quad (\text{II.5})$$

where

$$\mathbf{D}[\mathbf{u}] = \frac{1}{2} (\nabla \mathbf{u} + \nabla \mathbf{u}^T)$$

is the rate of strain and \mathbf{n} is the outward normal and $\boldsymbol{\mathcal{T}}[\mathbf{u}]$ is the integral of the moment of the traction vector.

▪ Weak Solution for the Total Momentum

Numerical solutions of the Navier-Stokes are expressed first in terms of a weak solution, which is in integral form and must be satisfied for all test functions in a certain space. The test functions are chosen to convert weak solutions to a matrix in which solutions are obtained at nodal points. In our work we use a special weak solution in which the fluid and particle equations of motion are combined into a *single weak equation of motion*, which governs the evolution of the *total momentum* of the system—fluid plus particles; the force $\mathbf{F}[\mathbf{u}]$ and torque $\boldsymbol{\mathcal{T}}[\mathbf{u}]$ cancel and do not need to be computed.

Find \mathbf{u} , p , \mathbf{U} , $\boldsymbol{\omega}$ and satisfying

$$\int_{fluid} \rho_f \left(\frac{\partial \mathbf{u}}{\partial t} + \mathbf{u} \cdot \nabla \mathbf{u} - \mathbf{g} \right) \cdot \mathbf{v} d\mathbf{x} - \int_{fluid} p \nabla \cdot \mathbf{v} d\mathbf{x} + \int_{fluid} 2\eta \mathbf{D}[\mathbf{u}] : \mathbf{D}[\mathbf{v}] d\mathbf{x} \quad (\text{II.6})$$

$$+ M \left(\frac{d\mathbf{U}}{dt} - \mathbf{g} \right) \cdot \mathbf{V} + I \frac{d\boldsymbol{\omega}}{dt} \cdot \boldsymbol{\xi} = 0 \quad \text{for all } \mathbf{v}, \mathbf{V}, \boldsymbol{\xi},$$

$$\int_{fluid} q \nabla \cdot \mathbf{u} d\mathbf{x} = 0 \quad \text{for all } q, \quad (\text{II.7})$$

where \mathbf{u} and \mathbf{v} are both required to satisfy the no-slip condition on the particle boundary:

$$\mathbf{u} = \mathbf{U} + \boldsymbol{\omega} \wedge \mathbf{r} \quad \mathbf{v} = \mathbf{V} + \boldsymbol{\xi} \wedge \mathbf{r}. \quad (\text{II.8})$$

The function spaces for the functions and test functions are described in papers where they are used.

The combined equation of motion (II.6), (II.7) and (II.8) in which hydrodynamic forces and torques are completely eliminated was introduced by Hesla 1991 and implemented first by Hu 1996.

The same type of methods can be used for viscoelastic liquids; of course the equations for the fluid motion are then different. For the Oldroyd-B fluids we have

$$\rho_f \frac{d\mathbf{u}}{dt} = -\nabla p + \text{div } \boldsymbol{\tau} \quad (\text{II.9})$$

$$\lambda_1 \overset{\nabla}{\boldsymbol{\tau}} + \boldsymbol{\tau} = 2\eta(\mathbf{D}[\mathbf{u}] + \lambda_2 \overset{\nabla}{\mathbf{D}}[\mathbf{u}]) \quad (\text{II.10})$$

where

$$\overset{\nabla}{(o)} = \frac{\partial(o)}{\partial t} + (\mathbf{u} \cdot \nabla)(o) - \nabla \mathbf{u} \cdot (o) - (o) \cdot \nabla \mathbf{u}^T \quad (\text{II.11})$$

is called the ‘‘upper convected derivative.’’ Here λ_1 , is a relaxation time and λ_2 is a retardation time. Newtonian fluids are recovered in the asymptotic limit $\lambda_2 \rightarrow \lambda_1$, $0 \leq \lambda_2 \leq \lambda_1$. It is convenient for simulation to write

$$\boldsymbol{\tau} = \boldsymbol{\tau}_E + 2\eta \mathbf{D}[\mathbf{u}] \quad (\text{II.12})$$

where

$$\boldsymbol{\tau}_E + \lambda_1 \overset{\nabla}{\boldsymbol{\tau}}_E = 2\eta_E \mathbf{D}[\mathbf{u}]. \quad (\text{II.13})$$

This leads to a formulation (III.1) of the problem in terms of the configuration tensor

$$\mathbf{A} = \boldsymbol{\tau}_E + \left(\frac{\eta_E}{\lambda_1} \right) \mathbf{1}.$$

III. Numerical Packages for Moving Particles in Direct Numerical Simulation

We developed two different kinds of numerical packages, called “particle movers,” one based on body fitted moving unstructured grids and another based on fixed structured grids over which bodies move by a method involving a system of Lagrange multipliers. Several different versions of each kind of code have been developed and tried on a variety of applications.

▪ ALE Particle Mover

Direct simulation of the motion of solid particles in fluids can be said to have started in the paper of Hu, Joseph and Crochet 1992a. The first method Hu *et al* 1992a uses an implicit update of the particle translational and angular velocities on unstructured grids (see figure III.1) to prevent numerical instability. This is achieved by alternately computing the hydrodynamic force and torque, then updating the particle translational and angular velocities using the equations of rigid-body motion, and iterating until the translational and angular velocities converge. The combined equations of motion (II.6, 7, 8) were used in Hu’s improved ALE scheme Hu 1996a, 2000 and Hu, Patankar and Zhu 2000.

The ALE particle mover uses a generalization of the standard Galerkin finite-element method on an unstructured body-fitted mesh, together with an Arbitrary Lagrangian-Eulerian (ALE) moving mesh technique to deal with the movement of particles (see, for example Hansbo 1992, Huerta and Liu 1988, Nomura and Hughes 1992). In our implementation, the nodes on a particle surface are assumed to move with the particle. The movement of the nodes in the interior of the fluid is computed using a modified Laplace’s equation, to ensure that they are smoothly distributed. At each time step, the grid is updated according to the motion of the particles. A new grid is generated whenever the elements of the mesh get too distorted, and the flow fields are projected onto the new grid.

The weak formulation of the ALE particle mover is based on (II.6, 7 and 8). These equations are reduced to algebraic equations by finite element methods on the unstructured grid like that in figure III.1. The strong form of these equations are the original equations (II.1 through 5) from which the weak form was derived.

Two versions of the ALE method are the integrated method introduced by H. Hu 1996a, and a splitting method implemented by H. Choi 2000. In the integrated method one solves for the velocity and pressure at the same time; in the splitting method one solves sequentially separate equations for the velocity and pressure.

The splitting method leads to a smaller system of equations than the integrated method; however, the divergence free condition is not enforced at every sequential step so that the velocity field which emerges from a divergence free step does not satisfy the momentum equation exactly; hence small time steps are required to solve the momentum equations with negligible error.

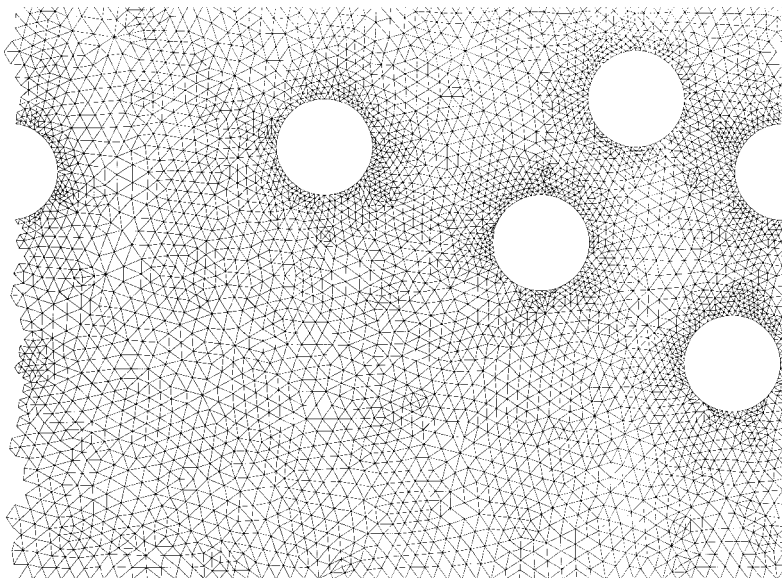


Figure III.1 Unstructured grid for the ALE method on a periodic domain.

The splitting method generates a symmetric saddle point matrix and leads to a symmetric positive definite pressure equation. The pressure gradient is solved by a conjugate gradient method without preconditioning because the matrixes involved are a composition of diagonally dominant matrices and other matrices conveniently formed with diagonal preconditioners. The methods run matrix-free of assembly of a global matrix.

▪ A Projected Particle Mover

Matt Knepley developed a variation of the ALE particle mover, Knepley, Sarin, Sameh 1998, in which the entire simulation is performed matrix-free in the space constrained to be discretely incompressible. Apart from the elegance of this approach, it simplifies the model by treating the particles and fluid in a decoupled fashion, and by eliminating pressure. The parallel multilevel preconditioner due to Sarin and Sameh 1998a, is used to obtain an explicit basis, P_v , for the discrete constrained divergence-free space. After elimination of pressure unknowns, a Krylov subspace method such as GMRES is used to solve the reduced system $P_v^T \tilde{A} P_v x = b$, where \tilde{A} is the constrained Jacobian for velocity unknowns. In contrast to the ALE particle mover discussed earlier, the linear systems in this method are positive-definite, and exhibit favorable convergence properties on account of the well-conditioned basis P_v . The algorithm has demonstrated very good scalability and efficiency for particle benchmarks on the SGI Origin 2000.

▪ DLM Particle Mover

The DLM particle mover uses a new Distributed-Lagrange-Multiplier-based fictitious-domain method. The basic idea is to imagine that fluid fills the space inside as well as outside the particle boundaries. The fluid-flow problem is then posed on a larger domain (the “fictitious domain”). This larger domain is simpler, allowing a simple regular mesh to be used. This in turn allows specialized fast solution techniques. The larger domain is also time-independent, so the *same* mesh can be used for the entire simulation, eliminating the need for repeated remeshing and projection (see figure III.2). This is a great advantage, since for three-dimensional particulate

flow the automatic generation of unstructured body-fitted meshes in the region outside a large number of closely spaced particles is a difficult problem. In addition, the entire computation is performed matrix-free, resulting in significant savings.

The velocity on each particle boundary must be constrained to match the rigid-body motion of the particle. In fact, in order to obtain a combined weak formulation with the hydrodynamic forces and torques eliminated, the velocity *inside* the particle boundary must also be a rigid-body motion. This constraint is enforced using a distributed Lagrange multiplier, which represents the additional body force per unit volume needed to maintain the rigid-body motion inside the particle boundary, much like the pressure in incompressible fluid flow whose gradient is the force required to maintain the constraint of incompressibility.

The scheme uses an operator-splitting technique for discretization in time. (Operator-splitting schemes have been used for solving the Navier-Stokes equations by many authors, starting, to our knowledge, with Chorin, 1967, 1968, and 1973, and Teman, 1997.) The linearly constrained quadratic minimization problems which arise from this splitting are solved using conjugate-gradient algorithms, yielding a method that is robust, stable, and easy to implement. For further details, see Glowinski, Pan, Hesla, Joseph and P eriaux 1999. The *immersed boundary method* of Peskin and his collaborators, Peskin 1997, 1981, Peskin and McQueen 1980, on the simulation of incompressible viscous flow in regions with elastic moving boundaries also uses a fictitious-domain method, but without Lagrange-multipliers.

The rigid motion constraint has been implemented in two ways leading to two codes, DLM1 and DLM2. The first implementation DLM1 Glowinski, Pan, Hesla and Joseph 1999 requires that the fluid at the places $P(t)$ occupied by the solid take on a rigid body velocity

$$\text{DLM1 } \mathbf{u}(\mathbf{x}, t) = \mathbf{U} + \boldsymbol{\omega} \wedge \mathbf{r}, \quad \mathbf{x} \in P(t)$$

where \mathbf{U} is the velocity of the mass center and $\boldsymbol{\omega} \wedge \mathbf{r}$ is the rotation around the mass center. The second implementation DLM2 Patankar, Singh, Joseph, Glowinski and Pan 2000 is stress-like, rigid motion on $P(t)$ is enforced by requiring that the rate of strain vanish there

$$\text{DLM2 } \mathbf{D}[\mathbf{u}] = 0, \quad x \in P(t)$$

where $\mathbf{D}[\mathbf{u}]$ is the symmetric part of $\nabla \mathbf{u}$.

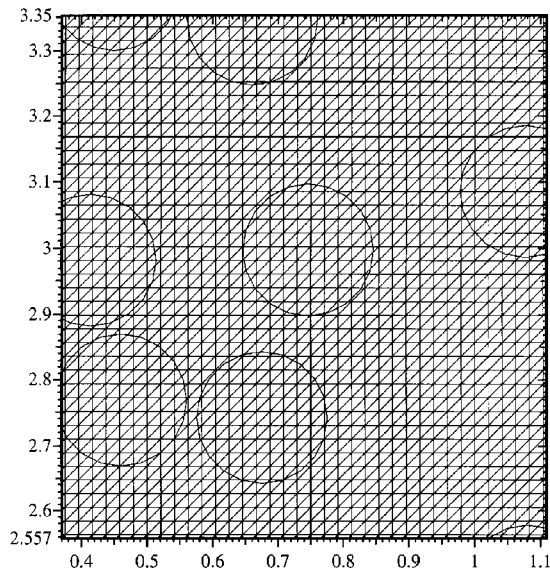


Figure III.2 Fixed triangular grid used in DLM computation. The same grid covers the fluid and solid. The fluid in the circles is bordered by Lagrange multipliers to move as a rigid body.

▪ Parallel Implementation

The DLM particle mover uses an operator-splitting technique consisting of three steps. In the first step, a saddle-point problem is solved using an Uzawa/conjugate-gradient algorithm, preconditioned by the discrete analogue of the Laplacian operator with homogeneous Neumann boundary conditions on the pressure mesh; such an algorithm is described in Turek 1996. The second step requires the solution of a non-linear discrete advection-diffusion problem that is solved by the algorithm discussed in Glowinski 1984. The third step solves another saddle-point problem using an Uzawa/conjugate-gradient algorithm.

The DLM approach uses uniform grids for two and three-dimensional domains, and relies on matrix-free operations on the velocity and pressure unknowns in the domain. This simplifies the distribution of data on parallel architectures and ensures excellent load balance (see Pan, Sarin, Glowinski, Sameh and Périaux 1999). The basic computational kernels, vector operations such as additions and dot products and matrix-free matrix-vector products, yield excellent scalability on distributed shared memory computers such as the SGI Origin 2000.

The main challenge in parallelization is posed by the solution of the Laplacian for the pressure mesh that functions as a preconditioner for the Uzawa algorithm. Fast solvers based on cyclic reduction for elliptic problems on uniform grids are overkill since the solution is required only to modest accuracy. A multilevel parallel elliptic solver, Sarin and Sameh 1998b, has been incorporated into the DLM algorithm. This has yielded speedup of over 10 for the preconditioning step on a 16 processor Origin.

The parallel DLM particle mover has been used to simulate the expansion of a fluidized bed discussed in chapter VII. Even though there is a serial component of the code, we have observed an overall speedup of 10 on the SGI Origin 2000 at NCSA, using 16 processors. In addition, this represents an impressive eight-fold increase in speed over the best serial implementation.

▪ Viscoelastic DLM Particle Mover

The ALE particle mover has been implemented for the popular Oldroyd-B constitutive model, which can be written in the form

$$\begin{aligned} \rho_f \left(\frac{\partial \mathbf{u}}{\partial t} + (\mathbf{u} \cdot \nabla) \mathbf{u} \right) &= -\nabla p + \nabla \cdot (2\eta \mathbf{D} + \mathbf{A}), \\ \nabla \cdot \mathbf{u} &= 0, \\ \lambda_1 \left(\frac{\partial \mathbf{A}}{\partial t} + (\mathbf{u} \cdot \nabla) \mathbf{A} - \mathbf{A} \cdot \nabla \mathbf{u} - \nabla \mathbf{u}^T \cdot \mathbf{A} \right) + \mathbf{A} &= \frac{\eta_E}{\lambda_1} \mathbf{1} \end{aligned} \quad (\text{III.1})$$

where \mathbf{D} is the rate-of-strain tensor, $\mathbf{A} = \tau_E + (\eta_E / \lambda_1) \mathbf{1}$ is the configuration tensor, τ_E is the elastic stress, η_E is the elastic viscosity, and λ_1 is the relaxation time. These equations are to be solved subject to appropriate boundary conditions.

The system (III.1) is classified mathematically as being of *composite* type, Joseph 1990a: The solution can have large gradients normal to the characteristic surfaces, which for this system are tangent to the streamlines. A numerical error in resolving these sharp gradients can cause one or more of the principal values of \mathbf{A} , which are always positive in the continuous problem, to become negative. This can cause a catastrophic amplification of short waves—a Hadamard instability, Singh and Leal 1993.

This Hadamard instability can be prevented by ensuring that \mathbf{A} remains positive-definite using a method introduced by Singh in Singh and Leal 1993, Singh and Leal 1994. The method has two key elements: a third-order upwinding scheme for discretizing the convection term in (II.10) and a time-dependent solution algorithm which explicitly forces the principal values of \mathbf{A} to be positive. The combination of these two elements ensures that the scheme will remain stable even at relatively large Deborah numbers. The equations are discretized in time using a second-order operator-splitting technique that decouples the constitutive equation from the incompressibility constraint. Singh, Joseph, Hesla, Glowinski and Pan 2000 have combined Singh's with the DLM method.

▪ Computation domains for pipe flows of slurries

In studying slurries and other pipe flows it is necessary to set the computational problem on a finite domain. It would be desirable to pose the problem as it is in nature using the end conditions. The problem posed this way requires knowledge of end conditions and the details of the motion may not determine the motion in the pipe, especially in long pipes. This same problem occurs in analysis of pipe flows in which a constant pressure gradient is prescribed as the ratio of the pressure drop Δp over the length L of pipe. The prescription of that constant pressure gradient is the only way in which the pressure drop is acknowledged. In analytical studies, the remaining nonconstant part of the pressure gradient can be posed in a suitable class of functions, say periodic in x . We could write

$$p(x, y, z, t) = Px + \Pi(x, y, z, t) \quad (\text{III.2})$$

where P is the constant pressure gradient and $\pi(x, y, z, t)$ is periodic with an assigned period in x . There are possibly different ways to choose this period and they are not equivalent. This is exactly where we are in simulation. We decompose the pressure as in (III.2), then we require that π and the velocity and other quantities are periodic in x with an assigned period. The assignment of the period is made decisively by the construction of a periodic mesh like the one shown in figure III.1. Clearly anything we compute on this mesh will have the assigned periodicity. The choice of periodicity and the selection of the period does cloud the relevance of computed to observed results and needs further study.

Simulations of single particle lift to equilibrium were also performed in a computational domain, which moves in the x -direction and is such that the particle is always at its center. The inflow and outflow boundaries are located at a specified distance from the center of the particle. A fully developed parabolic velocity profile $u(y) = \bar{p}y(W - y)/2\eta$ corresponding to the applied pressure gradient is imposed at the inflow and outflow boundaries.

▪ Collision Strategies

It is not possible to simulate the motion of even a moderately dense suspension of particles without a strategy to handle cases in which particles touch. In unstructured-grid methods, frequent near-collisions force large numbers of mesh points into the narrow gap between close particles and the mesh distorts rapidly, requiring an expensive high frequency of remeshing and projection. A “collision strategy” is a method for preventing near collisions while still conserving mass and momentum.

Four collision strategies are presently being used. They all define a security zone around the particle such that when the gap between particles is smaller than the security zone a repelling force is activated. A repelling force can be thought to represent surface roughness, for example. The repelling force pushes the particle out of the security zone into the region in which fluid forces computed numerically govern. The strategies differ in the nature of the repelling force and how it is computed. It is necessary to compare these different strategies.

A collision strategy for the ALE particle mover used by Hu 2000 chooses the repelling force so that the particles are forced just to the edge of the security zone. Another strategy for the ALE particle mover, due to Maury and Glowinski 1997, uses the lubrication force of Kim and Karrila 1991, to separate touching particles and it is also the only strategy that requires touching particles to transfer tangential as well as normal momentum. Maury and Glowinski developed his theory for smooth bodies of arbitrary shape.

A yet different collision strategy has been implemented for the DLM particle mover, Glowinski, Pan, Hesla and Joseph 1999. As in the other methods a security zone is defined. An explicit formula, linear in the distance of penetration into the security zone, is used to keep the particles apart. This repelling force may be tuned with a “stiffness” parameter.

Johnson and Tezduyar 1996, implemented a collision strategy based on the physics of inelastic collisions in which a security zone is defined by structured layers of elements around the particles. They model their strategy as an inelastic collision of elastic bodies with no fluid present and use the coefficient of restitution as a fitting parameter. The collision strategy is activated when the structured layers touch.

All of these strategies keep the particles farther apart than they ought to be, resulting in too high void fractions. To have real collision of smooth rigid particles it is necessary for the film between particles to rupture and film rupture requires physics and mathematics beyond the Navier-Stokes equations. Without film rupture physics, the best that can be expected from simulation is a strategy that allows for the action of lubrication forces to within the tolerance of the mesh.

This kind of "security zone free" scheme has been devised and implemented by Singh, Hesla and Joseph 2002. They modify the DLM method to allow the particles to come arbitrarily close to each other and even slightly overlap. When conflicting rigid body constraints from two different particles are applicable on a velocity node, the constraint from the particle that is closer to that node is used and the other constraint is dropped. An elastic repulsive force is applied when the particles overlap. The particles are allowed to overlap as much as one hundredth of the velocity element size.

The modified DLM method was applied for both Newtonian and viscoelastic liquids. Excellent results for particles in close approach and validation against analytical results were achieved.

IV. Weak and Strong Formulations of the DLM Method

The weak and strong forms of the equations for the DLM method are more interesting because the Lagrange multiplier field must be introduced. There are two ways to represent the rigid motion of a fluid in portions of the space occupied by solids; one way is to impose the condition that the velocity is given by the velocity of the mass center plus a rigid rotation, and the other is that on those portions of space, the rate of strain tensor vanishes. This gives rise to two versions of the DLM method: a body force formulation and a stress formulation.

▪ Body Force Formulation of DLM Method; Weak Solution

Find \mathbf{u} , p , $\boldsymbol{\lambda}$, \mathbf{U} and $\boldsymbol{\omega}$ satisfying

$$\int_{\Omega} \rho_f \left(\frac{\partial \mathbf{u}}{\partial t} + (\mathbf{u} \cdot \nabla) \mathbf{u} - \mathbf{g} \right) \cdot \mathbf{v} \, d\mathbf{x} \\ - \int_{\Omega} p \nabla \cdot \mathbf{v} \, d\mathbf{x} + \int_{\Omega} 2\eta \mathbf{D}[\mathbf{u}] : \mathbf{D}[\mathbf{v}] \, d\mathbf{x} \\ + \left(1 - \frac{\rho_f}{\rho_s} \right) \left(M \left(\frac{d\mathbf{U}}{dt} - \mathbf{g} \right) \cdot \mathbf{V} + \frac{d(I\boldsymbol{\omega} \cdot \boldsymbol{\xi})}{dt} \right)$$

, $\mathbf{H}_1(\Omega)$, p

$$= \int_{\Omega_s} \boldsymbol{\lambda} \cdot (\mathbf{v} - (\mathbf{V} + \boldsymbol{\xi} \wedge \mathbf{r})) \, d\mathbf{x} \quad , \quad \text{for all } \mathbf{u}, \mathbf{v} \text{ in } \mathbf{H}_1(\Omega), p \text{ and } \boldsymbol{\lambda} \text{ in } \mathbf{L}_2(\Omega), \mathbf{U}, \boldsymbol{\omega}, \mathbf{V}, \boldsymbol{\xi} \text{ in } \mathbf{R}^3 \quad (\text{IV.1})$$

$$\int_{\Omega_s} \mathbf{q} \nabla \cdot \mathbf{u} \, d\mathbf{x} = 0, \quad \mathbf{q} \in \mathbf{H}_1(\Omega) \quad (\text{IV.2})$$

$$\int_{\Omega_s} \boldsymbol{\mu} \cdot (\mathbf{u} - (\mathbf{U} + \boldsymbol{\omega} \wedge \mathbf{r})) \, d\mathbf{x}, \quad \boldsymbol{\mu} \in \mathbf{L}_2(\Omega) \quad (\text{IV.3})$$

Here $\boldsymbol{\lambda}(\mathbf{x}, t)$ is the Lagrange multiplier field, \mathbf{u} , p , $\boldsymbol{\lambda}$, \mathbf{U} and $\boldsymbol{\omega}$ are the unknown velocity, pressure, $\mathbf{U}(t)$ and $\boldsymbol{\omega}(t)$ are the velocity and angular velocity; $\mathbf{v}, \mathbf{V}, \boldsymbol{\xi}$ and $\boldsymbol{\mu}$ are the test functions, Ω_s is the domain occupied by solids, and $\Omega = \Omega_f \cup \Omega_s$ is the domain occupied by both fluid and solid, the entire domain shown as triangles in figure III.2.

▪ Body Force Formulation of DLM: Strong Solutions

Using standard methods of the calculus of variations, we obtain the strong form of the DLM equations of motion and constraint in fluids and solids. We get the Navier-Stokes over the whole

domain Ω but the Lagrange multiplier field appears only on the solid. We find that $\text{div } \mathbf{u} = 0$ on fluid and solid and

$$\rho_f \frac{d\mathbf{u}}{dt} = \rho_f \mathbf{g} + \nabla \cdot \boldsymbol{\sigma} + \boldsymbol{\lambda} \delta(\Omega_s) \quad (\text{IV.4})$$

where $\delta(\Omega_s)$ is one when $\mathbf{x} \in \Omega_s$ and zero otherwise and $\boldsymbol{\sigma} = -p\mathbf{1} + 2\eta\mathbf{D}[\mathbf{u}]$ is the stress. Here $\boldsymbol{\lambda} - a^2\nabla^2\boldsymbol{\lambda}$ is a body force. The solid is in rigid motion

$$\mathbf{u} = \mathbf{U} + \boldsymbol{\omega} \wedge \mathbf{r} \quad (\text{IV.5})$$

$\boldsymbol{\lambda}$ satisfies a natural boundary condition

$$(\mathbf{n} \cdot \nabla)\boldsymbol{\lambda} = \mathbf{n} \cdot (\boldsymbol{\sigma}_s - \boldsymbol{\sigma}_f) \quad (\text{IV.6})$$

evaluating (IV.4) in Ω_f , we find

$$\begin{aligned} \text{div } \mathbf{u} &= 0, \\ \rho_f \frac{d\mathbf{u}}{dt} &= \rho_f \mathbf{g} - \nabla p + \eta \nabla^2 \mathbf{u} \end{aligned} \quad (\text{IV.7})$$

in Ω_f and from (IV.5), using no-slip, we get

$$\mathbf{u} = \mathbf{U} + \boldsymbol{\omega} \wedge \mathbf{r} \quad \text{on } \partial\Omega_f. \quad (\text{IV.8})$$

Equation (IV.7) and (IV.8) are a Dirichlet problem when \mathbf{U} and $\boldsymbol{\omega}$ are given and the boundary of the particles defining $\partial\Omega_f$ are known; if all these “given” were known as a function of time we could solve any initial value problem in Ω_f without reference to $\boldsymbol{\lambda}(\mathbf{x}, t)$.

Using (IV.5) to evaluate (IV.4) on the solids Ω_s we get

$$\rho_f \left(\frac{d\mathbf{U}}{dt} + \frac{d\boldsymbol{\omega}}{dt} \wedge \mathbf{r} + \boldsymbol{\omega} \wedge (\boldsymbol{\omega} \wedge \mathbf{r}) - \mathbf{g} \right) = \boldsymbol{\lambda}. \quad (\text{IV.9})$$

Since there is no divergence constraint for $\boldsymbol{\lambda}$ we may put the pressure p in the solid to zero and, of course, $\mathbf{D}[\mathbf{u}] = 0$ on rigid motions, and

$$(\mathbf{n} \cdot \nabla)\boldsymbol{\lambda} = p\mathbf{n} - 2\eta\mathbf{D}[\mathbf{u}] \cdot \mathbf{n} \quad (\text{IV.10})$$

where p and \mathbf{u} are the values of these fields in the fluid on the $\partial\Omega_f$ of the solids. Once the fluid flow associated with (IV.7,8) is solved, the right side of (IV.10) is known and the linear equation (IV.9) may be solved for $\boldsymbol{\lambda}$. The $\boldsymbol{\lambda}$ field is selected to make the fluid on the domain Ω_s occupied by solids move as a rigid body.

In the weak solution, the position of $\Omega_s(t)$ are updated using Newton's equations (II.3) rigid bodies. The form of the equations (II.3) is specialized for spheres; for arbitrary shape Newton's equations of motion are more complicated.

▪ Stress Formulation of DLM: Weak Solutions

Patankar, Singh, Joseph, Glowinski and Pan 2000 have introduced a new formulation of the distributed Lagrange multiplier/fictitious domain method for particulate flows. In this formulation the deformation rate tensor in the fluid occupied by solids is constrained to be zero. The Lagrange multiplier field λ turns out to be a velocity and the mathematics gives rise to a stress like equation for λ in which the particle phase pressure may be put to zero.

The new formulation starts with the observation that on a rigid solid

$$\mathbf{D}[\mathbf{u}] = 0 \quad (\text{IV.11})$$

and a partial differential equation equivalent to (IV.11) is

$$\nabla \cdot \mathbf{D}[\mathbf{u}] = 0 \text{ in } \Omega_s \text{ and } \mathbf{D}[\mathbf{u}] \cdot \mathbf{n} = 0 \text{ on } \partial\Omega_s. \quad (\text{IV.12})$$

The combined form of the total momentum equation is formulated as follows:

Find $\mathbf{u}, p, \lambda, \mathbf{U}$ and $\boldsymbol{\omega}$ satisfying

$$\begin{aligned} \int_{\Omega} \rho_f \left(\frac{\partial \mathbf{u}}{\partial t} + (\mathbf{u} \cdot \nabla) \mathbf{u} - \mathbf{g} \right) \cdot \mathbf{v} \, d\mathbf{x} + \int_{\Omega} 2\eta \mathbf{D}[\mathbf{u}] : \mathbf{D}[\mathbf{v}] \, d\mathbf{x} - \int_{\Omega} p (\nabla \cdot \mathbf{v}) \, d\mathbf{x} + \int_{\Omega} q (\nabla \cdot \mathbf{u}) \, d\mathbf{x} \\ + \int_{\Omega_s} (\rho_s - \rho_f) \left(\frac{\partial \mathbf{u}}{\partial t} + (\mathbf{u} \cdot \nabla) \mathbf{u} - \mathbf{g} \right) \cdot \mathbf{v} \, d\mathbf{x} + \int_{\Omega_s} \mathbf{D}[\lambda] : \mathbf{D}[\mathbf{v}] \, d\mathbf{x} + \int_{\Omega_s} \mathbf{D}[\mathbf{u}] : \mathbf{D}[\mathbf{u}] \, d\mathbf{x} = 0 \end{aligned} \quad (\text{IV.13})$$

and

$$\begin{aligned} M\mathbf{U} &= \int_{\Omega_s} \rho_s \mathbf{u} \, d\mathbf{x} \\ \mathbf{I}\boldsymbol{\omega} &= \int_{\Omega_s} \mathbf{r} \times \rho_s \mathbf{u} \, d\mathbf{x}. \end{aligned} \quad (\text{IV.14})$$

▪ Stress Formulation of DLM: Strong Solutions

The strong form for (IV.13) may be found by the usual method of the calculus of variations. In Ω_f , we have $\text{div } \mathbf{u}=0$,

$$\rho_f \frac{d\mathbf{u}}{dt} = -\nabla p + \eta \nabla^2 \mathbf{u} + \rho_f \mathbf{g}. \quad (\text{IV.15})$$

In Ω_s , $\text{div } \mathbf{u}=0$, $\mathbf{D}[\mathbf{u}]=0$ and

$$\rho_s \frac{d\mathbf{u}}{dt} = -\nabla p + \eta \nabla^2 \mathbf{u} + \rho_s \mathbf{g} + \nabla \cdot \mathbf{D}[\boldsymbol{\lambda}]. \quad (\text{IV.16})$$

The velocity and stress traction vectors are continuous across $\partial\Omega_s = \partial\Omega_f$

$$\left. \begin{aligned} \mathbf{n} \cdot (-p_f \mathbf{1} + p_s \mathbf{1} + 2\eta \mathbf{D}[\mathbf{u}_f - \mathbf{u}_s]) &= \mathbf{n} \cdot \mathbf{D}[\boldsymbol{\lambda}], \\ \mathbf{u}_f &= \mathbf{u}_s. \end{aligned} \right\} \quad (\text{IV.17})$$

Noting next that (IV.5) holds in Ω_s and on $\partial\Omega_s$, we arrive again at the Dirichlet problem (IV.7) and (IV.8) for the Navier-Stokes equation in Ω_f . After putting $\mathbf{u} = \mathbf{U} + \boldsymbol{\omega} \wedge \mathbf{r}$ into (IV.16) and evaluating (IV.17), we get

$$\nabla \cdot (\mathbf{D}[\boldsymbol{\lambda}]) = \rho_s \left(\frac{d\mathbf{U}}{dt} + \frac{d\boldsymbol{\omega}}{dt} \wedge \mathbf{r} + \boldsymbol{\omega} \wedge (\boldsymbol{\omega} \wedge \mathbf{r}) - \mathbf{g} \right) \quad (\text{IV.18})$$

$$\mathbf{n} \cdot \mathbf{D}[\boldsymbol{\lambda}]_s = \mathbf{n} \cdot (-p\mathbf{1} + 2\eta \mathbf{D}[\mathbf{u}])_f. \quad (\text{IV.19})$$

This is a linear Dirichlet problem for $\boldsymbol{\lambda}$ when $\mathbf{U}(t)$, $\boldsymbol{\omega}(t)$ and the position of $\bar{\mathbf{X}}$ and $\boldsymbol{\theta}$ of the particles. This data determines \mathbf{u} and p in Ω_f through (IV.15) (or (VI.7)) and (IV.8).

$\mathbf{D}[\boldsymbol{\lambda}]$ is the rate of strain for the Lagrange multiplier velocity field $\boldsymbol{\lambda}$ in 3D and three equations (IV.18). It is *not* required that $\text{div } \boldsymbol{\lambda} = 0$; in general $\text{div } \boldsymbol{\lambda} \neq 0$. Hence a ‘‘pressure’’ field is not associated with $\boldsymbol{\lambda}$ field. We might frame this result for two-fluid models of solid-liquid flow which states the particle phase pressure vanishes.

A. Addendum to Chapter IV (Addendum A). Weak form of the body force formulation when the Lagrange multiplier is eliminated

Using equation (IV.9) and (IV.10), we may eliminate λ in the weak solution.[‡]

$$\int_{\Omega_s} \lambda \cdot (\mathbf{v} - (\mathbf{V} + \xi \wedge \mathbf{r})) dx = \rho_f \int_{\Omega_s} (\dot{\mathbf{U}} + \dot{\boldsymbol{\omega}} \wedge \mathbf{r} + \boldsymbol{\omega} \wedge (\boldsymbol{\omega} \wedge \mathbf{r}) - \mathbf{g}) \cdot (\mathbf{v} - (\mathbf{V} + \xi \wedge \mathbf{r})) dx \quad (\text{IV.20})$$

where

$$\dot{\mathbf{U}} = \frac{d\mathbf{U}}{dt}, \quad \dot{\boldsymbol{\omega}} = \frac{d\boldsymbol{\omega}}{dt}.$$

Noting now that $\Omega = \Omega/\Omega_s \cup \Omega_s$, where $\Omega/\Omega_s = \Omega_f$ is the part of Ω occupied by the fluid alone, we may write (IV.1), using (IV.20) as

$$\begin{aligned} & \int_{\Omega_f} \left\{ \rho_f \left[\frac{\partial \mathbf{u}}{\partial t} + (\mathbf{u} \cdot \nabla) \mathbf{u} - \mathbf{g} \right] \cdot \mathbf{v} + 2\eta \mathbf{D}[\mathbf{u}] : \mathbf{D}[\mathbf{v}] - p \nabla \cdot \mathbf{v} \right\} dx \\ & + \int_{\Omega_s} \rho_f \left[\frac{\partial \mathbf{u}}{\partial t} + (\mathbf{u} \cdot \nabla) \mathbf{u} - \dot{\mathbf{U}} - \dot{\boldsymbol{\omega}} \wedge \mathbf{r} - \boldsymbol{\omega} \wedge (\boldsymbol{\omega} \wedge \mathbf{r}) \right] \cdot \mathbf{v} dx \\ & + \left(1 - \frac{\rho_f}{\rho_s} \right) \left[M (\dot{\mathbf{U}} - \mathbf{g}) \cdot \mathbf{V} + \frac{d}{dt} (\mathbf{I} \boldsymbol{\omega}) \cdot \xi \right] \\ & + \rho_f \int_{\Omega_s} [\dot{\mathbf{U}} + \dot{\boldsymbol{\omega}} \wedge \mathbf{r} + \boldsymbol{\omega} \wedge (\boldsymbol{\omega} \wedge \mathbf{r}) - \mathbf{g}] \cdot (\mathbf{V} + \xi \wedge \mathbf{r}) dx = 0, \end{aligned} \quad (\text{IV.21})$$

where

$$\mathbf{I} = \rho_s \int_{\Omega_s} [r^2 \mathbf{1} - \mathbf{r} \otimes \mathbf{r}] dx$$

is the moment of inertia tensor.

The position vector \mathbf{r} is measured from the mass center of the particle. Since ρ_s is uniform, the volume and mass centers are identical and

$$\int_{\Omega_s} \mathbf{r} dx = 0 \quad (\text{IV.22})$$

where $\mathbf{r} = \mathbf{x} - \mathbf{X}(t)$ and \mathbf{X} is the center of mass.

Using (IV.22), we may simplify and rewrite the last term of (IV.21) as

[‡] I'm indebted to Todd Hesla for his help with the reduction of the weak to strong solution and some of the calculations leading to (IV.25).

$$\rho_f (\dot{\mathbf{U}} - \mathbf{g}) \cdot \mathbf{V} \int_{\Omega_s} dx + \rho_f \int_{\Omega} [\dot{\boldsymbol{\omega}} \wedge \mathbf{r} + \boldsymbol{\omega} \wedge (\boldsymbol{\omega} \wedge \mathbf{r})] (\boldsymbol{\xi} \wedge \mathbf{r}) dx .$$

Noting next that $M = \rho_s \int_{\Omega_s} dx$, the terms proportional to \mathbf{V} in (IV.21) are

$$M[\dot{\mathbf{U}} - \mathbf{g}] \cdot \mathbf{V}$$

and the terms proportional to $\boldsymbol{\xi}$ become

$$\left(1 - \frac{\rho_f}{\rho_s}\right) \frac{d}{dt} (\mathbf{I}\boldsymbol{\omega}) \cdot \boldsymbol{\xi} + \rho_f \int_{\Omega} [\dot{\boldsymbol{\omega}} \wedge \mathbf{r} + \boldsymbol{\omega} \wedge (\boldsymbol{\omega} \wedge \mathbf{r})] (\boldsymbol{\xi} \wedge \mathbf{r}) dx$$

which, after applying well known vector identities, becomes

$$\left(1 - \frac{\rho_f}{\rho_s}\right) \frac{d}{dt} (\mathbf{I}\boldsymbol{\omega}) \cdot \boldsymbol{\xi} + \rho_f \int_{\Omega_s} [\mathbf{r}^2 \dot{\boldsymbol{\omega}} - (\mathbf{r} \cdot \dot{\boldsymbol{\omega}}) \mathbf{r} + \boldsymbol{\omega} \cdot \mathbf{r} (\mathbf{r} \wedge \boldsymbol{\omega})] \cdot \boldsymbol{\xi} dx$$

or

$$\left(1 - \frac{\rho_f}{\rho_s}\right) \frac{d}{dt} (\mathbf{I}\boldsymbol{\omega}) \cdot \boldsymbol{\xi} + \frac{\rho_f}{\rho_s} (\mathbf{I}\dot{\boldsymbol{\omega}}) \cdot \boldsymbol{\xi} + \frac{\rho_f}{\rho_s} \boldsymbol{\omega} \wedge (\mathbf{I}\boldsymbol{\omega}) \cdot \boldsymbol{\xi} . \quad (\text{IV.23})$$

We note next that

$$\frac{d}{dt} (\mathbf{I}\boldsymbol{\omega}) = \mathbf{I}\dot{\boldsymbol{\omega}} + \rho_s \int_{\Omega_s} [\boldsymbol{\omega} (\mathbf{r} \cdot \frac{d\mathbf{r}}{dt}) - (\boldsymbol{\omega} \cdot \frac{d\mathbf{r}}{dt}) \mathbf{r} - (\boldsymbol{\omega} \cdot \mathbf{r}) \frac{d\mathbf{r}}{dt}] dx .$$

Since

$$\frac{d\mathbf{r}}{dt} = \left[\frac{\partial}{\partial t} + (\mathbf{U} + \boldsymbol{\omega} \wedge \mathbf{r}) \cdot \nabla \right] [\mathbf{x} - \mathbf{X}(t)] = -\dot{\mathbf{X}} + \mathbf{U} + \boldsymbol{\omega} \wedge \mathbf{r} = \boldsymbol{\omega} \wedge \mathbf{r} ,$$

this reduces to

$$\frac{d}{dt} (\mathbf{I}\boldsymbol{\omega}) = \mathbf{I}\dot{\boldsymbol{\omega}} + \boldsymbol{\omega} \wedge (\mathbf{I}\boldsymbol{\omega}) . \quad (\text{IV.24})$$

After inserting (IV.24) into (IV.23), all of the terms except $\boldsymbol{\xi} \cdot d(\mathbf{I}\boldsymbol{\omega})/dt$ vanish. The terms proportional to \mathbf{V} and $\boldsymbol{\xi}$ in (IV.21) therefore simplify drastically to

$$M[\dot{\mathbf{U}} - \mathbf{g}] \cdot \mathbf{V} + \frac{d}{dt} (\mathbf{I}\boldsymbol{\omega}) \cdot \boldsymbol{\xi} .$$

The reformulated statement of the weak form of our solid liquid system is obtained after eliminating λ from (IV.1) by the method just given. The combined momentum formulation, fluid plus solid, is

$$\begin{aligned} & \int_{\Omega_f} \rho_f \left[\frac{\partial \mathbf{u}}{\partial t} + (\mathbf{u} \cdot \nabla) \mathbf{u} - \mathbf{g} \right] \cdot \mathbf{v} dx + \int_{\Omega_f} \{ 2\eta \mathbf{D}[\mathbf{u}] : \mathbf{D}[\mathbf{v}] - p \nabla \cdot \mathbf{v} \} dx \\ & + \int_{\Omega_s} \rho \left[\frac{\partial \mathbf{u}}{\partial t} + (\mathbf{u} \cdot \nabla) \mathbf{u} - \dot{\mathbf{U}} - \dot{\boldsymbol{\omega}} \wedge \mathbf{r} - \boldsymbol{\omega} \wedge (\boldsymbol{\omega} \wedge \mathbf{r}) \right] \cdot \mathbf{v} dx \\ & + M(\dot{\mathbf{U}} - \mathbf{g}) \cdot \mathbf{V} + \frac{d}{dt} (\mathbf{I} \boldsymbol{\omega}) \cdot \boldsymbol{\xi} = 0, \end{aligned} \quad (\text{IV.25})$$

where the test functions $\mathbf{v} \in \mathbf{H}^1(\Omega)^3$ and $\mathbf{V} \in R^3$ and $\boldsymbol{\xi} \in R^3$ are vectors. The integral on Ω_s guarantees that the momentum on of the patches of fluid Ω_s on places occupied by the solids is for a rigid body motion. The fluid is weakly solenoidal

$$\int_{\Omega} q \nabla \cdot \mathbf{u} dx = 0, \quad q \in L^2(\Omega)$$

and the condition

$$\int_{\Omega_s} \boldsymbol{\mu} \cdot [\mathbf{u} - (\mathbf{U} + (\boldsymbol{\omega} \wedge \mathbf{r}))] dx = 0, \quad \boldsymbol{\mu} \in \mathbf{H}^1(\Omega)^3$$

guarantees that the fluid moves as a rigid body.